

Efficient joint noise removal and multi exposure fusion

A. Buades¹, J.L Lisani¹, O. Martorell^{1*}

1 Institute of Applied Computing and Community Code (IAC3) and with the Dept.of Mathematics and Computer Science, Universitat de les Illes Balears, Cra. de Valldemossa km. 7.5, E-07122 Palma, Spain

¶The authors acknowledge the Ministerio de Ciencia, Innovación y Universidades (MCIU), the Agencia Estatal de Investigación (AEI) and the European Regional Development Funds (ERDF) for its support to the project TIN2017-85572-P.

* o.martorell@uib.cat

Abstract

Multi-exposure fusion (MEF) is a technique for combining different images of the same scene acquired with different exposure settings into a single image. All the proposed MEF algorithms combine the set of images, somehow choosing from each one the part with better exposure.

We propose a novel multi-exposure image fusion chain taking into account noise removal. The novel method takes advantage of DCT processing and the multi-image nature of the MEF problem. We propose a joint fusion and denoising strategy taking advantage of spatio-temporal patch selection and collaborative 3D thresholding. The overall strategy permits to denoise and fuse the set of images without the need of recovering each denoised exposure image, leading to a very efficient procedure.

1 Introduction

Multi-exposure fusion (MEF) is a technique for combining different images of the same scene acquired with different exposure settings into a single image. By keeping the best exposed parts of each image, we can recover a single image where all features are well represented. Compared to High Dynamic Range (HDR), MEF avoids the estimation of the camera response function and the tone mapping, keeping during all the process the original range of the images.

All the proposed MEF algorithms combine the set of images, somehow choosing from each one the part with better exposure. Most methods express this choice as a combination of pixel values or their gradient, commonly weighted depending on exposure, saturation and contrast, e.g. Mertens et al. [41]. In order to make this choice robust, the methods use a pyramidal structure or work at the patch level instead of the pixel one. In

the case that pixel gradient is manipulated, a final estimate has to be recovered by Poisson editing [47].

Image fusion is an extensive research area not limited to multi-exposure images. The combination of several images permits to improve their quality, removing for example noise [6], compression artifacts [15], haze [21], blur [54] or shaking blur from hand held video [10],[9].

We propose a novel multi-exposure image fusion chain taking into account noise removal. Instead of combining gradients or pixel values, we fuse the Discrete Cosinus Transform (DCT) coefficients of the differently exposed images. The use of the DCT permits to include a thresholding stage attenuating noise during the fusion process. DCT thresholding is a well known method for noise removal, behaving extremely well with moderate noise levels and being efficient in terms of computational complexity. We propose a novel strategy taking advantage of DCT thresholding and the multi-image nature of the MEF problem.

The methods in [37] and [40] propose a similar fusion procedure to ours. However, they do not include any noise removal stage. The method in Ma et al. [37] uses a patch based approach, in which each patch is decomposed into its average and detail patch. Averages are combined depending on exposure, while detail patches are averaged depending on its magnitude. Our approach also deals differently with the average and the details but it uses DCT to represent the details and not just the difference of the patch with its average. While the method in [37] is applied to each color channel, we use a color decorrelation transform.

The method in [40] uses a DCT transform but instead of combining the averages of the patches it uses an auxiliary image obtained with Mertens et al [41] algorithm to set the patch illumination. We combine the average coefficients depending on local and global exposure. The method in [40] applies a completely different strategy for luminance and chromatic parts, while our method uses the same procedure for both components, permitting noise reduction.

Although the proposed fusion method is able to deal with low levels of noise, for more challenging cases the simple DCT thresholding might be insufficient. Based on noise removal methods for image and video [8, 6], we propose a joint strategy taking advantage of spatio-temporal patch selection [6] and collaborative 3D thresholding [8]. The computed patch DCTs for collaborative thresholding are directly fed into the fusion procedure. The overall strategy permits to denoise and fuse the set of images without the need of recovering each denoised exposure image, leading to a very

fast procedure.

Section 2 describes the MEF existing literature. The proposed method for the fusion of images with different exposures is described in Section 3. Section 4 presents the complete method including the fusion and noise removal stages. In Section 5, we discuss the implementation of the method and compare with state of the art algorithms and we draw some conclusions in Section 6.

2 Related work

Several MEF methods have been proposed in the literature. Mertens et al. [41] proposed a pixel wise combination of images depending on contrast, saturation and well-exposedness. Many algorithms appeared improving aspects of their method or making it motion adaptive, such as Li et al. [31], An et al. [3], Ocampo et al. [44], Liu et al. [35], Hayat et al. [16] and Hessel et al. [18].

Another type of methods combine the gradient of the images, and then they recover the solution by Poisson image editing [47]. For several algorithms, just the most convenient gradient is chosen, for example Kuk et al. [25]. Other methods combine all gradients, for example [53, 63, 13, 57].

Instead of fusing red, green and blue values, the YCbCr [11] color space is often used. Paul et al. [46] combines the luminance using a gradient based fusion. The chromatic components are fused by direct pixel-wise averaging favoring colored pixels compared to gray ones. A similar approach is adopted in [40].

This pixel-wise choice is not robust enough and needs to be regularized by using pyramidal structures or working at the patch level. The Laplacian pyramid proposed by Burt and Adelson [7] was adopted by Mertens et al. [42] and posterior methods Ancuti et al. [4], Kou et al. [24, 23]. Patch-based methods use as minimal unit small image windows, which makes them more robust than pixel wise algorithms since much more values are involved in the fusion process (Goshtasby [12], Zhang et al. [64], Zhang et al. [65], Ma et al. [37]).

When the image sequence is not completely static, the fusion of moving objects creates a ghosting effect. There exist three main strategies to avoid these artifacts. The first strategy is to take into account block distance or correlation in order to weight the combination process. Such a weighted average might discard moving objects from the combination. The second one is to modify the sequence to make it static [20, 34, 67, 40]. A third straightforward strategy, adopted by several algorithms [58, 50, 55, 19], is to fuse several instances of the same reference image. The image with middle exposure is chosen as reference and is photometrically matched to each of the rest. These copies of the reference are then fused by any MEF method. This strategy permits to get rid of motion

and misalignments, but does not use the detail and structure information of the rest of images, only their color distribution.

Several methods (Z. G. Li et al. [33, 32], Singh et al. [56], Raman et al. [52], Li et al. [30]) separate low frequency (base images) from high frequency (detail images) using the Bilateral filter [59] or the Guided filter [17]. This separation permits an additional enhancement of the detail part.

Variational methods [48, 5, 14] have also been proposed to model MEF fusion. The proposed energies prefer to keep the geometry of the short exposure images and the color distribution of the long ones. The methods [38, 26, 36] try to optimize a quality measure of the final estimate. Ma et al. [36] proposed to optimize a modification of the objective quality measure in [39], adapted to color images.

Neural network methods have recently appeared for MEF and HDR imaging. Prabhakar et al. [51] uses a loss function minimizing an exposure fusion objective metric [39], avoiding the creation of ground truth images for the learning phase. Prabhakar et al. [49] proposed a neural network to align differently exposed images and merge them. Kalantari et al. [22] and Wu et al. [60] proposed learning methods for HDR imaging. Both networks apply to sequences of three images, and for the learning phase they need the corresponding LDR and HDR pairs for the three images. The main difference between both methods is that in [22] the input images are aligned by an optical flow estimation and warping, whereas in [60] the images do not need to be aligned before being introduced to the network.

Zhang et al. [66] and Xu et al. [61] proposed a unified deep learning framework for several fusion tasks, including MEF. Zhang et al. [66] extract features using convolutional layers, which are combined using an elementwise operation (mean for multi-exposure images). The final result is reconstructed from the fused features by additional convolutional layers. Xu et al. [61] trained a neural network to preserve the adaptive similarity between the fusion result and source exposures, that is, not requiring the ground truth images. Li et al. (CNNFEAT) [29] use CNN to extract features, which are used to combined the different exposures. However, the fused result is not the direct output of a neural network.

There is very few literature dealing with noise removal during multi exposure image fusion, and most published papers are focused on HDR. Akyuz et al. [2] denoise each frame before fusion, but this is performed in the radiance domain. Tico et al. [58] combines an initial fusion with the image of the sequence with the shortest exposure in the luminance domain. This combination is performed in the wavelet domain and coefficient attenuation is applied to the coefficients of the difference of luminances. Min et al. [43] filter the set of images by spatio-temporal motion compensated anisotropic filters prior to HDR reconstruction.

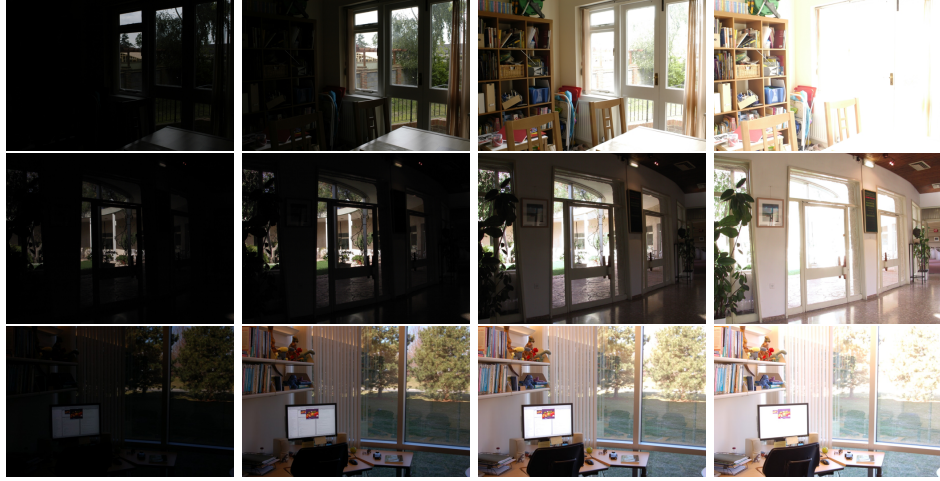


Figure 1: Multi exposure data sets used for comparison.

Lee et al. [28] use sub-band architecture for fusion, with a weighted combination using a motion indicator function to avoid ghosting effects. The low frequency bands are filtered with a multi-resolution bilateral filter while the high frequency bands are filtered by soft thresholding. Ahmad et al. [1] identify noisy pixels and reduce their weight during image fusion.

3 Proposed fusion algorithm

We propose a novel algorithm for multi-exposure fusion adopting the Fourier aggregation model as main tool.

3.1 Single Channel image fusion

Let assume we have a multi-exposure sequence of image luminance, supposed to be pre-registered, which we denote by Y_k , $k = 1, 2, \dots, K$. Since each image might contain well exposed areas, we apply the combination locally. We split the images Y_k into partially-overlapped blocks of $b \times b$ pixels, $\{B_k^l\}$, $l = 1, \dots, n_b$, n_b the number of blocks.

Both under and over exposed patches will have Fourier coefficients of smaller magnitude, due to the lack of high frequency information; while well exposed patches will have Fourier coefficients of larger magnitude. We propose to fuse the non-zero frequencies of each block as follows:

$$\hat{B}^l(\xi) = \sum_{k=1}^K w_k^l(\xi) \hat{B}_k^l(\xi), \quad \xi \neq 0, \quad l = 1, 2, \dots, n_b, \quad (1)$$

where \hat{B}_k^l denotes the DCT transform of patch l in image k , and the weights $w_k^l(\xi)$ are defined depending on ξ ,

$$w_k^l(\xi) = \frac{|\hat{B}_k^l(\xi)|^p}{\sum_{n=1}^K |\hat{B}_n^l(\xi)|^p} \quad \xi \neq 0. \quad (2)$$

The parameter p controls the weight of each Fourier mode.

This strategy does not apply to the zero frequency Fourier coefficient, $\xi = 0$, i.e. the mean. Since large zero frequency coefficients correspond to over-exposed images, applying the same weighted combination would simply overexpose the fused image. We weight these coefficients depending on how exposed is the local patch, as well as the entire image, with respect to the other ones.

$$\hat{B}^l(0) = \sum_{k=1}^K w_k^l(0) \hat{B}_k^l(0), \quad l = 1, 2, \dots, n_b,$$

where

$$w_k^l(0) = \frac{1}{C} e^{-(\hat{B}_k^l(0) - 0.5)^2 / \sigma_l^2} \cdot e^{-(\mu_k - 0.5)^2 / \sigma_g^2}, \quad (3)$$

with μ_k the average of image k , C a normalizing constant, and σ_l and σ_g parameters of the method. The averages of the patches are normalized to $[0, 1]$, then 0.5 corresponds to the gray level mid value.

Finally, applying the inverse DCT transform to each block we obtain the fused blocks.

$$B^l(x) = \mathcal{F}^{-1}(\hat{B}^l(\xi)), \quad l = 1, \dots, n_b. \quad (4)$$

Since blocks are partially overlapped, the pixels in overlapping areas are averaged to produce the final image.

3.2 Color image fusion

We use an orthonormal chromatic version of the well known YUV space, described by the following linear transformation.

$$\begin{pmatrix} Y \\ U \\ V \end{pmatrix} = \begin{pmatrix} \frac{1}{\sqrt{3}} & \frac{1}{\sqrt{3}} & \frac{1}{\sqrt{3}} \\ \frac{\sqrt{2}}{2} & 0 & -\frac{\sqrt{2}}{2} \\ \frac{1}{\sqrt{6}} & -\frac{2}{\sqrt{6}} & \frac{1}{\sqrt{6}} \end{pmatrix} \begin{pmatrix} R \\ G \\ B \end{pmatrix}$$

The Y channel, given by the average of the RGB values, represents the luminance, while U and V contain the chromatic information. The use of an orthonormal



Figure 2: Comparison between applying the fusion to each RGB channel independently and using the YUV luminance and chromatic components. The luminance of the two results is identical, while the color is enhanced by the latter strategy.

transform is motivated by the denoising stage described below.

The channel Y is processed as exposed above, with the average coefficient combined depending on exposure. However, for the U and V components, we use the weighted average defined by Equations (1) and (2) for all coefficients, including $\xi = 0$.

The use of such a weighting does not increase the risk of over-exposure, but enhances the patch average chromaticity, making the result more colorful than when applying the single channel method to each of the components R, G and B. This is noticeable in Fig. 2, in which both strategies are compared.

3.3 Noise removal

Assuming a classical Gaussian uniform white noise scenario with standard deviation σ , the proposed fusion method can naturally incorporate noise removal. By modifying the weight definition (2) to

$$w_k^l(\xi) = \frac{Thr_\sigma(|\hat{B}_k^l(\xi)|)^p}{\sum_{n=1}^K Thr_\sigma(|\hat{B}_n^l(\xi)|)^p}, \quad \xi \neq 0 \quad (5)$$

where

$$Thr_\sigma(|\hat{B}_k^l(\xi)|) = \begin{cases} 0 & |\hat{B}_k^l(\xi)| < T \cdot \sigma \\ |\hat{B}_k^l(\xi)| & \text{otherwise} \end{cases}$$

Since the YUV color transformation is orthonormal, the noise standard deviation is not modified by the linear transformation converting from RGB to the mentioned space. Thus, the same thresholding can be applied to each channel. The parameter T is set to 2.7 as usual when denoising by thresholding in an orthonormal basis.

Fig. 3 compares the application of the fusion chain with and without this DCT thresholding stage.

When dealing with high levels of noise, the DCT thresholding method described above is not enough to provide good denoising results. The next section describes how the fusion method can be combined with a collaborative denoising technique to obtain much better results.

4 Joint noise removal and fusion procedure

We assume as in the previous sections, that data is static and a uniform white noise model of standard deviation σ . Many variants have been proposed to deal with the noise removal of image sequences having the same exposure and noise conditions. Such methods cannot be directly used for MEF.

We propose a joint noise removal and fusion procedure (see scheme in Fig. 4). The noise removal stage uses a collaborative DCT thresholding as in [8], and a spatio-temporal patch selection as in [6]. The spatio-temporal selection permits a more robust patch comparison. The use of collaborative DCT thresholding permits a natural integration with the proposed fusion method, since both denoising and fusion are performed in the DCT domain, thus avoiding the need to reconstruct each denoised image prior to the fusion step.

The proposed strategy is well adapted to the MEF framework, namely to the fact that all the images have different exposure. In the patch-selection process, only patches belonging to the same image are compared, thus avoiding computing the similarity of patches with different exposure. In the same line, only patches having the same exposure are used in the denoising step.

Given the static image sequence, we build 3D blocks of patches, composed by the 2D patches from the sequence located at the same spatial position. The distance between different 3D blocks is computed as

$$d_{3D}(\mathbf{x}, \mathbf{y}) = \sum_{\text{image } i \text{ in sequence}} ||P_i(\mathbf{x}) - P_i(\mathbf{y})||$$

where $P_i(\mathbf{x})$ and $P_i(\mathbf{y})$ denote the 2D patches referenced by \mathbf{x} and \mathbf{y} in image i (each 2D patch is referenced by its top-left vertex).

By selecting the k nearest neighboring 3D blocks, we actually select k patches for each exposure. Collaborative DCT thresholding (see [8, 27]) is applied separately to the selected 2D patches belonging to the same exposure image.

The above collaborative filtering recovers the denoised DCT patches which are fed directly into the fusion procedure. That is, the proposed algorithm does

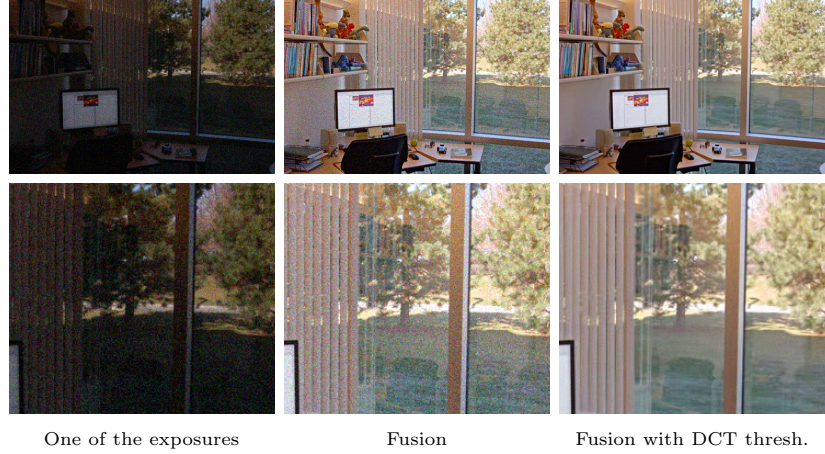


Figure 3: Noisy example with sequence Office and noise standard deviation 15. Top and from left to right: one image from the exposures set, fused without and with DCT thresholding. Below: detail of the images.

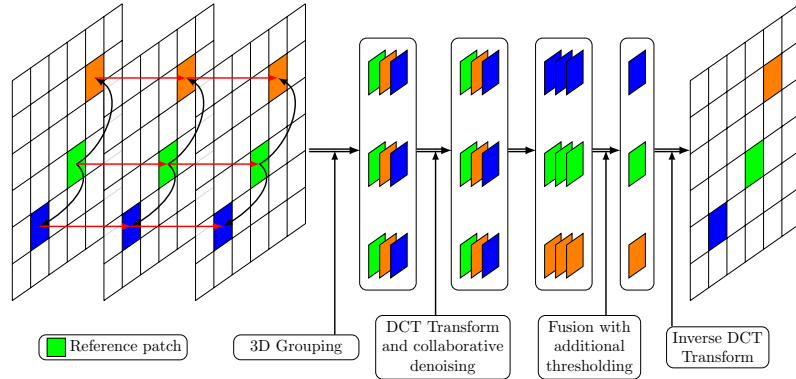


Figure 4: Processing scheme of a specific reference patch.

not need to apply the 2D inverse DCT to the grouped patches in order to recover each denoised exposure.

Each 3D block of the k selected ones contains denoised 2D DCT patches corresponding at the same spatial location and different exposure. Each one is combined by the fusion process which includes the additional DCT thresholding. The inverse DCT is applied to the k fused patches, which permits an additional aggregation in the image domain.

The joint patch selection procedure reduces the dependence of noise in patch comparison, improving the robustness of the method and reducing the usual artifacts of collaborative filtering.

5 Discussion and experimental results

In this section we compare the proposed method with state of the art algorithms for exposure fusion. We compare with Mertens et al. [41], Ma et al. [37], Li et al. [32], Kou et al. [23], Ma et al. [36], Hessel et al. (EEF) [18], Paul et al. [45], Zhang et al. (IFCNN) [66], Li et al. (CNNFEAT) [29], Hayat et al. (MEF-

Sift) [16] and Martorell et al. [40]. The results from Ma et al. [37] and Ma et al. [36] were computed with the software downloaded from the corresponding author's webpage. The results of Mertens et al. [41] were obtained from the dataset provided in [62] and [39]. The code for Hessel et al.¹ (EEF) [18], Paul et al.² [46], Zhang et al.³ (IFCNN) [66], Li et al.⁴ (CNNFEAT) [29] and Hayat et al.⁵ (MEF-Sift) [16] were obtained from corresponding github webpage. The results from Li et al. [32], Kou et al. [23] and Martorell et al. [40] were computed with the code provided by the authors. In all cases, default parameter settings are adopted.

Our results were computed using the same parameters for all tests in this section. We use blocks of size 8×8 pixels and $p = 7$ as the power exponent of the coefficient magnitudes in Equation 2. A sliding window approach is applied for the DCT based denosing/fusion. Once it is processed, the window is moved along both directions with a displacement step of $N_{step} = 2$. The

¹http://www.ipol.im/pub/art/2019/278/?utm_source=doi

²<https://github.com/sujoyp/gradient-domain-imagefusion>

³<https://github.com/uzeful/IFCNN>

⁴<https://github.com/xiaohuiben/MEF-CNN-feature>

⁵<https://github.com/ImranNust/Source-Code>

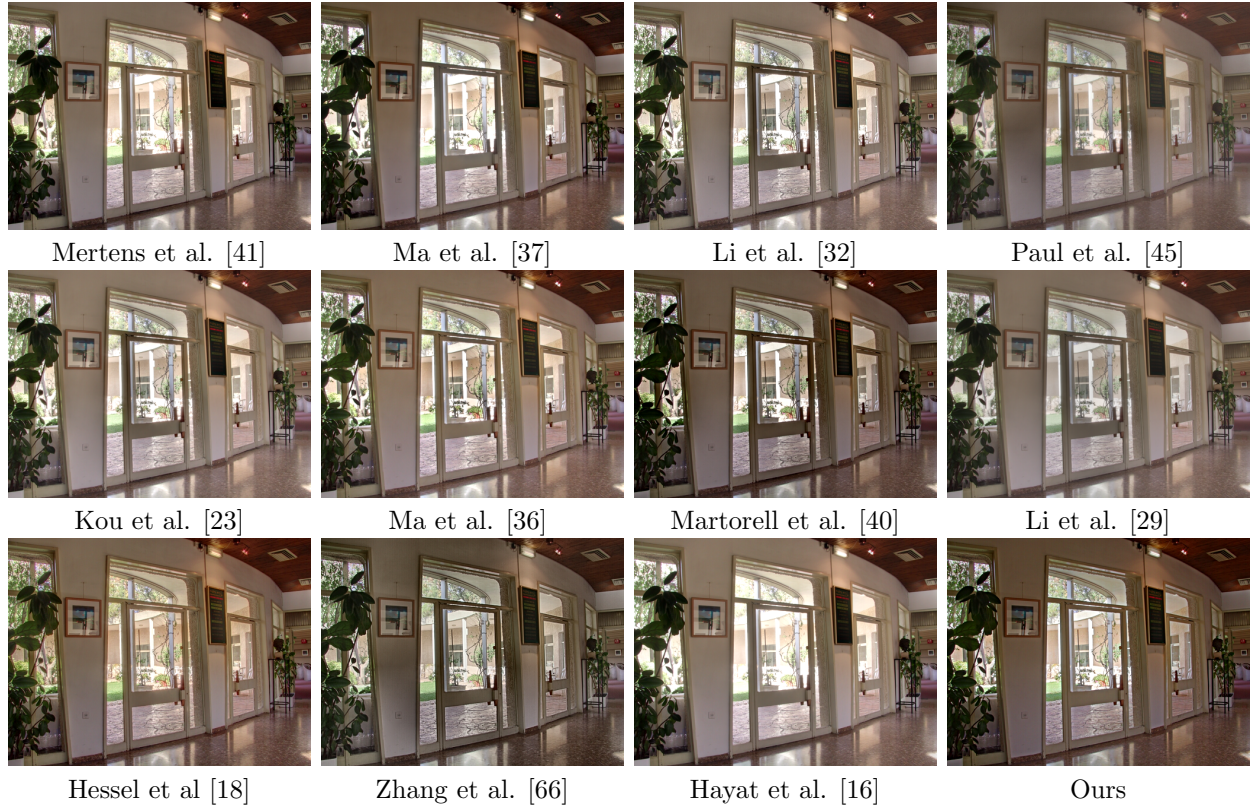


Figure 5: Results of fusion of noise-free multi-exposure images with different methods.

fact that the whole window is fused permits the processing of all the pixels in the image.

5.1 Noise free sequences

In this case, we just compare the ability of fusing the different exposure images. We use for our method just the fusion algorithm described in section 3, but without applying any thresholding of the DCT. Note that none of the compared methods include this noise filtering step.

Fig. 5 displays the results of all the methods on the “Belgium House” data set. Most methods have a good global illumination. However, looking closer to the details in Fig. 6, we might observe that many outdoor details in Mertens et al. [41] and Ma et al. [37] are overexposed, losing its definition. Li et al. [32] and Kou et al. [23] are not able to maintain the letters on the blackboard on the right side of Fig. 6 and Ma et al. [36] is not able to preserve the details on the tree at the top of the detail image. Li et al. [29] fusion is over-smoothed, while the result by Hayat et al. [16] is over-saturated at bright parts. The result of [40], Hessel et al [18], Zhang et al. [66] and ours are quite similar.

5.2 Noisy sequences with white uniform Gaussian Noise

We compare in Fig. 8 all the algorithms on a noisy multi exposure sequence with standard deviation of 15.

We apply all the algorithms with their default parameters. It is clear from this figure, that the rest of methods are not adapted or do not take into account noise.

In Fig. 10 we add noise of standard deviation 25 to each exposure and apply the BM3D algorithm [8] to denoise each image. We apply the different multi exposure fusion methods to the denoised data. Our method is applied directly to the noisy sequence.

The zoom of an extract, Fig. 11, shows that our method is the only one able to denoise and fuse the multi exposure sequence without noticeable artifacts.

5.3 Realistic multi exposure noisy images

We finally test our fusion and noise removal method with a realistic noise case. We add a signal dependent noise at each RAW image of the multi exposure set. We then apply a standard demosaicking, color processing, gamma correction and compression to the noisy raw images. The result is a realistic set of noisy multi exposure color images.

We apply our denoising and fusion algorithm to these images. The result is displayed in Fig. 12.

5.4 Computational analysis

The time complexity of the proposed algorithm is $\mathcal{O}(|Y|)$, where $|Y|$ denotes the size of each image in the multi-exposure sequence.

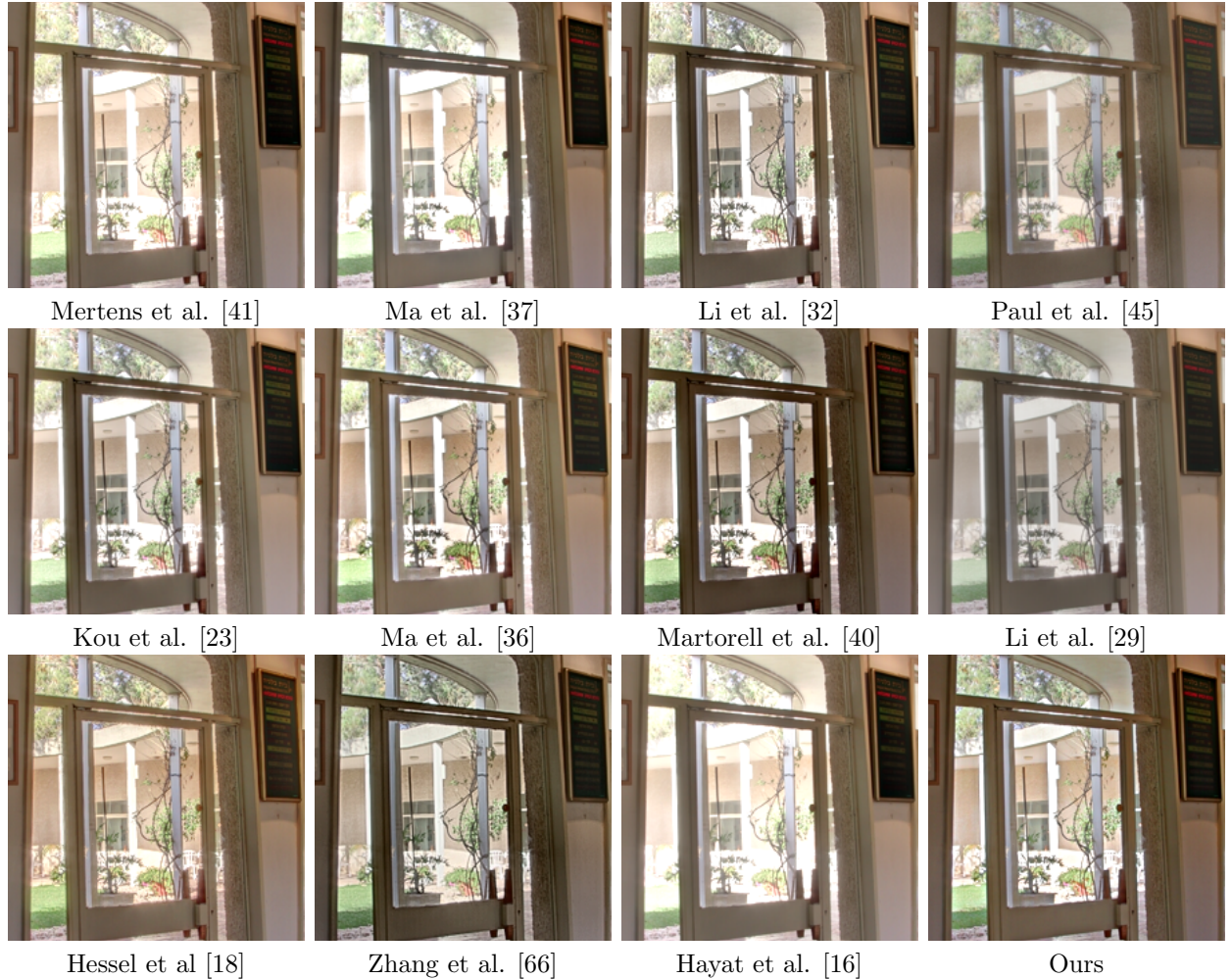


Figure 6: Extract of the results shown in Fig. 5.

Assuming that the 3D transforms used for the collaborative filtering are performed in a separable way (i.e. 2D transforms followed by 1D transforms, as detailed in [8]), the overall number of operations of the algorithm, per pixel, is approximately

$$\mathcal{C}_{\mathcal{T}_{2D}} + 2Kb^2N_S^2 + 2Kb^2\mathcal{C}_{\mathcal{T}_{1D}} + 2Kkb^2 + k\mathcal{C}'_{\mathcal{T}_{2D}} + kb^2 \quad (6)$$

where:

- $\mathcal{C}_{\mathcal{T}_{2D}}$ denotes the number of operations required to compute the 2D DCT of the block of patches similar to the one centered at the considered pixel. If we consider a neighborhood of size $N_S \times N_S$ around the pixel, this implies the computation of KN_S^2 2D DCTs, where K is the number of images in the sequence. The time complexity can be reduced by pre-computing the transforms in each block of size $K \times N_S \times N_S$ and reusing them in overlapping blocks, similarly to what is proposed in [8].

- The second term accounts for the 3D block matching step. This implies the exhaustive search, in a $N_S \times N_S$ neighborhood of the pixel, of 3D blocks of size $K \times b \times b$.

- The third term counts the number of operations for the computation of the 1D DCT transforms (direct and inverse) of the k nearest neighbors of each patch, in each frame. $\mathcal{C}_{\mathcal{T}_{1D}}$ denotes the cost of computing a 1D DCT transform (direct or inverse) of a vector of size k .
- The fourth term accounts for the fusion step, which involves k 3D blocks of patches of size $K \times b \times b$.
- The fifth term accounts for the number of operations needed to compute the k inverse 2D DCT transforms of the fused patches. $\mathcal{C}'_{\mathcal{T}_{2D}}$ denotes the cost of computing the inverse 2D DCT transform of a patch of $b \times b$ pixels.
- Finally, the last term counts the number of operations involved in the aggregation step.

Observe that the number of denoising operations per pixel, for each image, is smaller than that of BM3D since only one step of the collaborative filtering is applied. In addition, the inverse DCT is applied only to fused patches, since denoised exposures are not required by the algorithm.

Moreover, the previous estimation assumes that an exhaustive-search algorithm has been used for block matching. The costs \mathcal{C}_T of the DCT transforms depends on the availability of fast algorithms. By using predictive search techniques and fast separable transforms the complexity of the algorithm could be significantly reduced. Moreover, the overall number of operations can be further reduced by processing only one out of each $N_{\text{step}} < b$ pixels in both the horizontal and vertical directions. Due to the overlapping of the patches, the aggregation step used in the final step of the algorithm guarantees that all the pixels are correctly processed. In this case, the overall complexity of the method is reduced by a factor N_{step}^2 .

6 Conclusions

In this paper we propose a patch-based method for the simultaneous denoising and fusion of a sequence of multi-exposure images. Both tasks are performed in the DCT domain and take advantage of a collaborative 3D thresholding approach similar to BM3D [8] for denoising, and of the state-of-the-art fusion technique proposed in [40]. For the collaborative denoising, a spatio-temporal criterion is used to select similar patches along the sequence, following the approach in [6]. The overall strategy permits to denoise and fuse the set of images without the need of recovering each denoised exposure image, leading to a very efficient procedure.

Several experiments show that the proposed method permits to obtain state-of-the-art fusion results even when the input multi-exposure images are noisy. As future work, we plan to extend the current approach to multi exposure video sequences.

Acknowledgments

The authors thank Zhenguo Li and Fei Kou for kindly providing the implementation of [32] and [23], respectively.

References

- [1] Attiq Ahmad, Muhammad Mohsin Riaz, Abdul Ghafoor, and Tahir Zaidi. Noise resistant fusion for multi-exposure sensors. *IEEE Sensors Journal*, 16(13):5123–5124, 2016.
- [2] Ahmet Oğuz Akyüz and Erik Reinhard. Noise reduction in high dynamic range imaging. *Journal of Visual Communication and Image Representation*, 18(5):366–376, 2007.
- [3] Jaehyun An, Sang Heon Lee, Jung Gap Kuk, and Nam Ik Cho. A multi-exposure image fusion algorithm without ghost effect. In *Acoustics, Speech and Signal Processing (ICASSP)*, 2011 IEEE International Conference on, pages 1565–1568. IEEE, 2011.
- [4] Codruta O Ancuti, Cosmin Ancuti, Christophe De Vleeschouwer, and Alan C Bovik. Single-scale fusion: An effective approach to merging images. *IEEE Transactions on Image Processing*, 26(1):65–78, 2017.
- [5] Marcelo Bertalmio and Stacey Levine. Variational approach for the fusion of exposure bracketed pairs. *IEEE Transactions on Image Processing*, 22(2):712–723, 2013.
- [6] Antoni Buades, Jose-Luis Lisani, and Marko Miladinović. Patch-based video denoising with optical flow estimation. *IEEE Transactions on Image Processing*, 25(6):2573–2586, 2016.
- [7] Peter J. Burt and Edward H. Adelson. The laplacian pyramid as a compact image code. *IEEE TRANSACTIONS ON COMMUNICATIONS*, 31:532–540, 1983.
- [8] Kostadin Dabov, Alessandro Foi, Vladimir Katkovnik, and Karen Egiazarian. Image denoising by sparse 3-d transform-domain collaborative filtering. *IEEE Transactions on image processing*, 16(8):2080–2095, 2007.
- [9] M. Delbracio and G. Sapiro. Hand-Held Video Deblurring Via Efficient Fourier Aggregation. *Computational Imaging, IEEE Transactions on*, 1(4):270–283, Dec 2015.
- [10] M. Delbracio and G. Sapiro. Removing Camera Shake via Weighted Fourier Burst Accumulation. *Image Processing, IEEE Transactions on*, 24(11):3293–3307, Nov 2015.
- [11] Rafael C Gonzalez and Richard E Wood. *Digital image processing*, 2nd edtn.
- [12] A. A. Goshtasby. Fusion of multi-exposure images. *Image Vision Comput.*, 23(6):611–618, June 2005.
- [13] Bo Gu, Wujing Li, Jiangtao Wong, Minyun Zhu, and Minghui Wang. Gradient field multi-exposure images fusion for high dynamic range image visualization. *Journal of Visual Communication and Image Representation*, 23(4):604 – 610, 2012.
- [14] David Hafner and Joachim Weickert. Variational exposure fusion with optimal local contrast. In *International Conference on Scale Space and Variational Methods in Computer Vision*, pages 425–436. Springer, 2015.
- [15] Gloria Haro, Antoni Buades, and Jean-Michel Morel. Photographing paintings by image fusion. *SIAM Journal on Imaging Sciences*, 5(3):1055–1087, 2012.



Figure 7: Noisy multi-exposure data sets used for comparison. On the first row, the noise standard deviation of each input image is 15. On the second row the standard deviation is 25.



Figure 8: Results of fusion of noisy multi-exposure images with different methods. The noise standard deviation of each input image is 15.

- [16] Naila Hayat and Muhammad Imran. Ghost-free multi exposure image fusion technique using dense sift descriptor and guided filter. *Journal of Visual Communication and Image Representation*, 62:295 – 308, 2019.
- [17] Kaiming He, Jian Sun, and Xiaou Tang. Guided image filtering. *IEEE transactions on pattern analysis and machine intelligence*, 35(6):1397–1409, 2013.
- [18] Charles Hessel. Extended Exposure Fusion. *Image Processing On Line*, 9:453–468, 2019.
- [19] Jun Hu, Orazio Gallo, and Kari Pulli. Exposure stacks of live scenes with hand-held cameras. *Computer Vision–ECCV 2012*, pages 499–512, 2012.
- [20] Jun Hu, Orazio Gallo, Kari Pulli, and Xiaobai Sun. Hdr deghosting: How to deal with saturation? In *Proceedings of the IEEE Conference on Computer Vision and Pattern Recognition*, pages 1163–1170, 2013.
- [21] Neel Joshi and Michael F Cohen. Seeing mt. rainier: Lucky imaging for multi-image denoising, sharpening, and haze removal. In *Computational Photography (ICCP), 2010 IEEE International Conference on*, pages 1–8. IEEE, 2010.
- [22] Nima Khademi Kalantari and Ravi Ramamoorthi. Deep high dynamic range imaging of dynamic

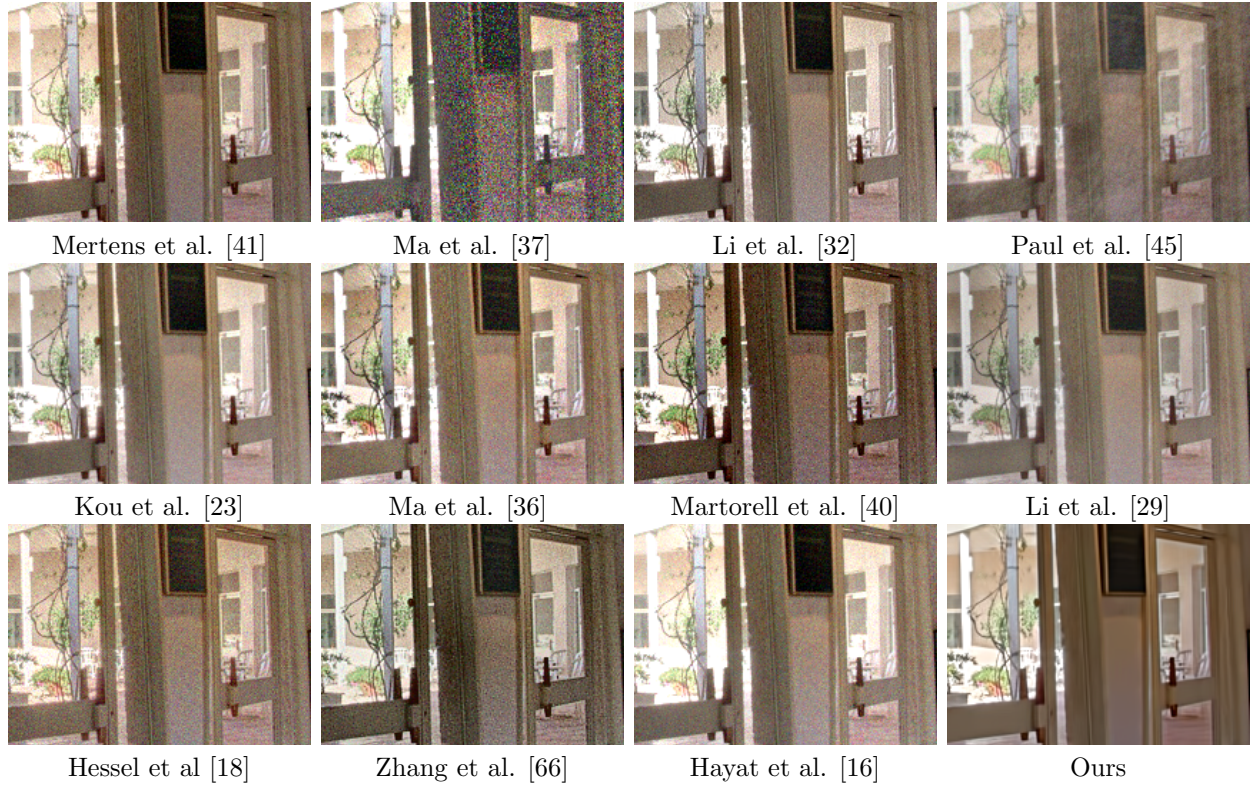


Figure 9: Extract of the results shown in Fig. 8. It is clear from this figure, that our method is the only one that takes noise into account

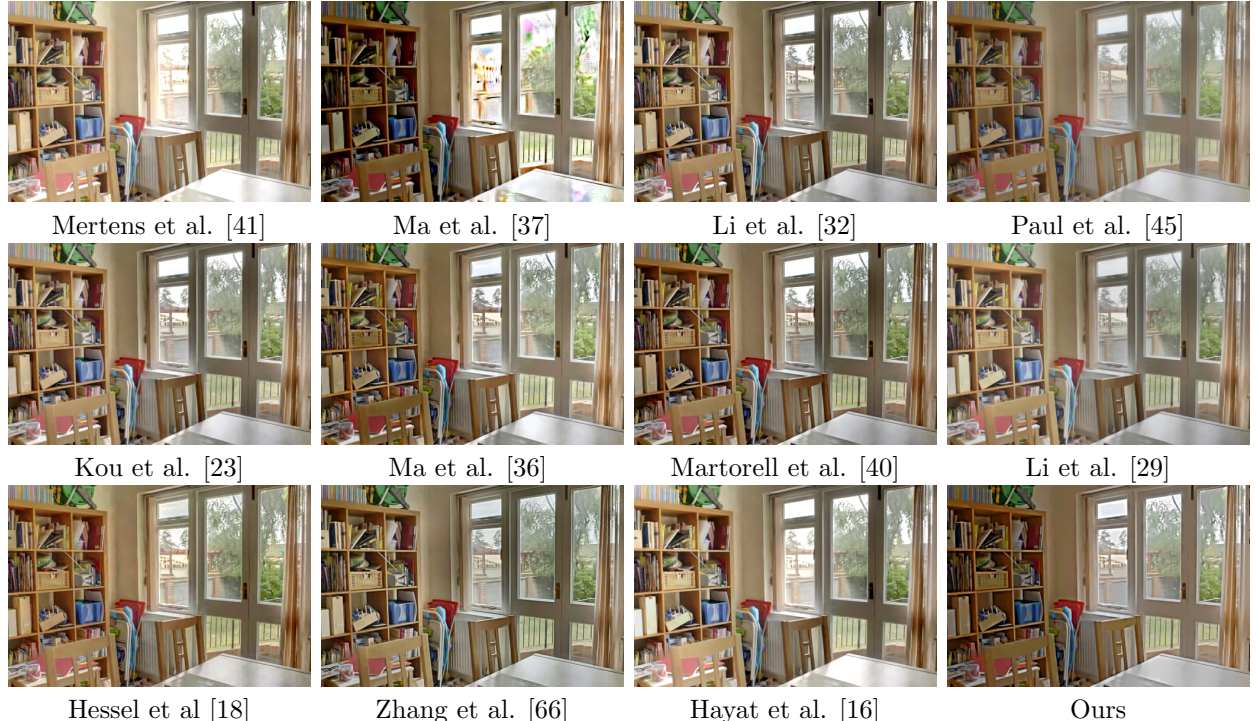


Figure 10: Results of fusion and denoising. Our method is the only one applied directly to the noisy multi-exposure images. The rest of methods fuse denoised versions of the images obtained using the BM3D algorithm. The noise standard deviation of each input image is 25.

scenes. *ACM Trans. Graph.*, 36(4):144–1, 2017.

[23] Fei Kou, Zhengguo Li, Changyun Wen, and Wei-

hai Chen. Multi-scale exposure fusion via gradient domain guided image filtering. In *2017 IEEE International Conference on Multimedia and Expo*

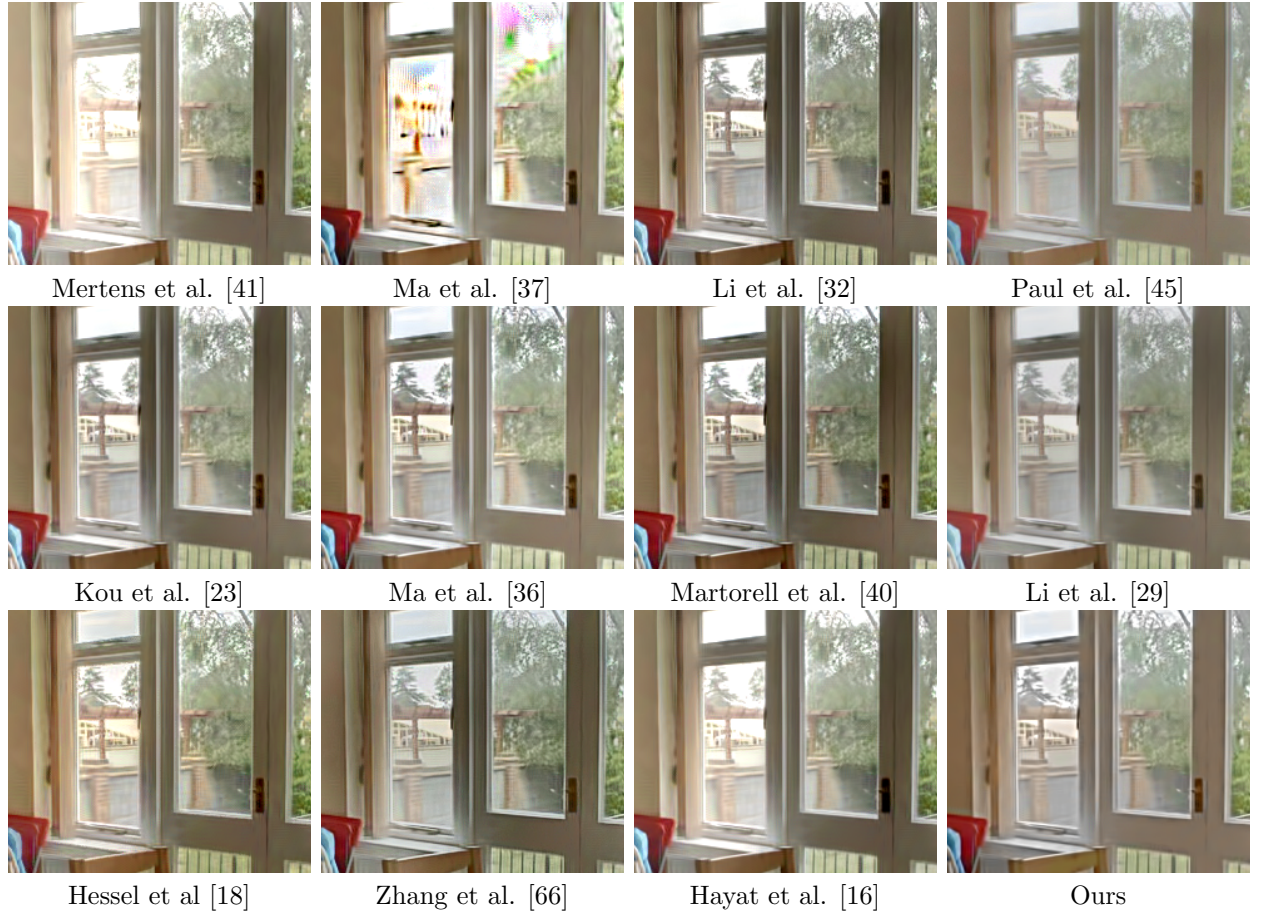


Figure 11: Extract of the results shown in Fig. 10.



Figure 12: Realistic noise simulation. From left to right: three exposure noisy images and the fusion and noise removal result. Below an extract of each image.

(ICME), pages 1105–1110. IEEE, 2017.

[24] Fei Kou, Zhengguo Li, Changyun Wen, and Weihai Chen. Edge-preserving smoothing pyramid based multi-scale exposure fusion. *Journal of Visual Communication and Image Representation*, 53:235–244, 2018.

[25] Jung Gap Kuk, Nam Ik Cho, and Sang Uk Lee. High dynamic range (hdr) imaging by gradient domain fusion. In *Acoustics, Speech and Signal Processing (ICASSP), 2011 IEEE International Conference on*, pages 1461–1464. IEEE, 2011.

[26] Valero Laparra, Alexander Berardino, Johannes

Ballé, and Eero P Simoncelli. Perceptually optimized image rendering. *JOSA A*, 34(9):1511–1525, 2017.

[27] Marc Lebrun. An Analysis and Implementation of the BM3D Image Denoising Method. *Image Processing On Line*, 2:175–213, 2012. <https://doi.org/10.5201/ipol.2012.1-bm3d>.

[28] Dong-Kyu Lee, Rae-Hong Park, and Soonkeun Chang. Ghost and noise removal in exposure fusion for high dynamic range imaging. *International Journal of Computer Graphics & Animation*, 4(4):1, 2014.

[29] H. Li and L. Zhang. Multi-exposure fusion with cnn features. In *2018 25th IEEE International Conference on Image Processing (ICIP)*, pages 1723–1727, 2018.

[30] S. Li, X. Kang, and J. Hu. Image fusion with guided filtering. *IEEE Trans. Image Processing*, 22(7):2864–2875, 2013.

[31] Shutao Li and Xudong Kang. Fast multi-exposure image fusion with median filter and recursive filter. *IEEE Transactions on Consumer Electronics*, 58(2), 2012.

[32] Z. Li, Z. Wei, C. Wen, and J. Zheng. Detail-enhanced multi-scale exposure fusion. *IEEE Transactions on Image Processing*, 26(3):1243–1252, March 2017.

[33] Z. G. Li, J. H. Zheng, and S. Rahardja. Detail-enhanced exposure fusion. *IEEE Trans. Image Processing*, 21(11):4672–4676, 2012.

[34] Zhengguo Li, Jinghong Zheng, Zijian Zhu, and Shiqian Wu. Selectively detail-enhanced fusion of differently exposed images with moving objects. *IEEE Transactions on Image Processing*, 23(10):4372–4382, 2014.

[35] Yu Liu and Zengfu Wang. Dense sift for ghost-free multi-exposure fusion. *Journal of Visual Communication and Image Representation*, 31:208–224, 2015.

[36] Kede Ma, Zhengfang Duanmu, Hojatollah Yeganeh, and Zhou Wang. Multi-exposure image fusion by optimizing a structural similarity index. *IEEE Transactions on Computational Imaging*, 4(1):60–72, 2018.

[37] Kede Ma, Hui Li, Hongwei Yong, Zhou Wang, Deyu Meng, and Lei Zhang. Robust multi-exposure image fusion: A structural patch decomposition approach. *IEEE Trans. Image Processing*, 26(5):2519–2532, 2017.

[38] Kede Ma, Hojatollah Yeganeh, Kai Zeng, and Zhou Wang. High dynamic range image compression by optimizing tone mapped image quality index. *IEEE Transactions on Image Processing*, 24(10):3086–3097, 2015.

[39] Kede Ma, Kai Zeng, and Zhou Wang. Perceptual quality assessment for multi-exposure image fusion. *IEEE Transactions on Image Processing*, 24(11):3345–3356, 2015.

[40] Onofre Martorell, Catalina Sbert, and Antoni Buades. Ghosting-free dct based multi-exposure image fusion. *Signal Processing: Image Communication*, 78:409–425, 2019.

[41] T. Mertens, J. Kautz, and F. Van Reeth. Exposure Fusion: A Simple and Practical Alternative to High Dynamic Range Photography. *Computer Graphics Forum*, 2009.

[42] Tom Mertens, Jan Kautz, and Frank Van Reeth. Exposure fusion. In *Proceedings of the 15th Pacific Conference on Computer Graphics and Applications*, PG '07, pages 382–390, Washington, DC, USA, 2007. IEEE Computer Society.

[43] Tae-Hong Min, Rae-Hong Park, and SoonKeun Chang. Noise reduction in high dynamic range images. *Signal, Image and Video Processing*, 5(3):315–328, 2011.

[44] Cristian Ocampo-Blandon and Yann Gousseau. Non-local exposure fusion. In *Iberoamerican Congress on Pattern Recognition*, pages 484–492. Springer, 2016.

[45] Sujoy Paul, Ioana S. Sevcenco, and P. Agathoklis. Multi-exposure and multi-focus image fusion in gradient domain. *J. Circuits Syst. Comput.*, 25:1650123:1–1650123:18, 2016.

[46] Sujoy Paul, Ioana S Sevcenco, and Panajotis Agathoklis. Multi-exposure and multi-focus image fusion in gradient domain. *Journal of Circuits, Systems and Computers*, 25(10):1650123, 2016.

[47] Patrick Pérez, Michel Gangnet, and Andrew Blake. Poisson image editing. In *ACM Transactions on graphics (TOG)*, volume 22, pages 313–318. ACM, 2003.

[48] Gemma Piella. Image fusion for enhanced visualization: A variational approach. *International Journal of Computer Vision*, 83(1):1–11, 2009.

[49] K Ram Prabhakar, Rajat Arora, Kunal Pratap Singh, and R Venkatesh Babu. A fast, scalable and reliable deghosting method for extreme exposure fusion. In *2019 IEEE International Conference on Computational Photography (ICCP)*. IEEE, 2019.

[50] K Ram Prabhakar and R Venkatesh Babu. Ghosting-free multi-exposure image fusion in gradient domain. In *Acoustics, Speech and Signal Processing (ICASSP), 2016 IEEE International Conference on*, pages 1766–1770. IEEE, 2016.

[51] K Ram Prabhakar, V Sai Srikanth, and R Venkatesh Babu. Deepfuse: A deep unsupervised approach for exposure fusion with extreme exposure image pairs. In *ICCV*, pages 4724–4732, 2017.

[52] Shanmuganathan Raman and Subhasis Chaudhuri. Bilateral Filter Based Compositing for Variable Exposure Photography. In P. Alliez and M. Magnor, editors, *Eurographics 2009 - Short Papers*. The Eurographics Association, 2009.

[53] Ramesh Raskar, Adrian Ilie, and Jingyi Yu. Image fusion for context enhancement and video surrealism. In *ACM SIGGRAPH 2005 Courses*, page 4. ACM, 2005.

[54] Alex Rav-Acha and Shmuel Peleg. Two motion-blurred images are better than one. *Pattern recognition letters*, 26(3):311–317, 2005.

[55] Wei-Rong Sie and Chiou-Ting Hsu. Alignment-free exposure fusion of image pairs. In *Image Processing (ICIP), 2014 IEEE International Conference on*, pages 1802–1806. IEEE, 2014.

[56] H. Singh, V. Kumar, and S. Bhooshan. A novel approach for detail-enhanced exposure fusion using guided filter. *The Scientific World Journal*, 2014(659217):8, 2014.

[57] Jian Sun, Hongyan Zhu, Zongben Xu, and Chongzhao Han. Poisson image fusion based on markov random field fusion model. *Information fusion*, 14(3):241–254, 2013.

[58] Marius Tico, Natasha Gelfand, and Kari Pulli. Motion-blur-free exposure fusion. In *Image Processing (ICIP), 2010 17th IEEE International Conference on*, pages 3321–3324. IEEE, 2010.

[59] Carlo Tomasi and Roberto Manduchi. Bilateral filtering for gray and color images. In *Computer Vision, 1998. Sixth International Conference on*, pages 839–846. IEEE, 1998.

[60] Shangzhe Wu, Jiarui Xu, Yu-Wing Tai, and Chi-Keung Tang. Deep high dynamic range imaging with large foreground motions. In *Proceedings of the European Conference on Computer Vision (ECCV)*, pages 117–132, 2018.

[61] Han Xu, Jiayi Ma, Junjun Jiang, Xiaojie Guo, and Haibin Ling. U2fusion: A unified unsupervised image fusion network. *IEEE Transactions on Pattern Analysis and Machine Intelligence*, 2020.

[62] Kai Zeng, Kede Ma, R. Hassen, and Z. Wang. Perceptual evaluation of multi-exposure image fusion algorithms. In *2014 Sixth International Workshop on Quality of Multimedia Experience (QoMEX)*, pages 7–12, Sept 2014.

[63] Wei Zhang and Wai-Kuen Cham. Gradient-directed multiexposure composition. *IEEE Transactions on Image Processing*, 21(4):2318–2323, 2012.

[64] Wei Zhang, Shengnan Hu, and Kan Liu. Patch-based correlation for deghosting in exposure fusion. *Information Sciences*, 415:19–27, 2017.

[65] Wei Zhang, Shengnan Hu, Kan Liu, and Jian Yao. Motion-free exposure fusion based on inter-consistency and intra-consistency. *Information Sciences*, 376:190–201, 2017.

[66] Yu Zhang, Yu Liu, Peng Sun, Han Yan, Xiaolin Zhao, and Li Zhang. Ifcnn: A general image fusion framework based on convolutional neural network. *Information Fusion*, 54:99 – 118, 2020.

[67] Jinghong Zheng and Zhengguo Li. Superpixel based patch match for differently exposed images with moving objects and camera movements. In *2015 IEEE International Conference on Image Processing (ICIP)*, pages 4516–4520. IEEE, 2015.